Effect of the Berendsen thermostat on dynamical properties of water

Anirban Mudi and Charusita Chakravarty*

Department of Chemistry, Indian Institute of Technology-Delhi, New Delhi: 110016, India.

* Author for correspondence (Tel: (+) 91 11 26591510; Fax: (+) 91 11 2651 6459; E-mail: charus@chemistry.iitd.ernet.in)

Abstract

The effect of the Berendsen thermostat on the dynamical properties of bulk SPC/E water is tested by generating power spectra associated with fluctuations in various observables. The Berendsen thermostat is found to be very effective in preserving temporal correlations in fluctuations of tagged particle quantities over a very wide range of frequencies. Even correlations in fluctuations of global properties, such as the total potential energy, are well-preserved for time periods shorter than the thermostat time constant. Deviations in dynamical behaviour from the microcanonical limit do not, however, always decrease smoothly with increasing values of the thermostat time constant but may be somewhat larger for some intermediate values of τ_B, specially in the supercooled regime, which are similar to time scales for slow relaxation processes in bulk water.

The ideal ensemble to extract dynamical information from a molecular dynamics simulation is the microcanonical (NVE) ensemble [1, 2]. Since the total energy is conserved in this ensemble, the Newtonian equations of motion can be assumed to represent the natural evolution of the system, subject to the accuracy of using classical mechanics to describe the atomic dynamics. The constant energy (E) and volume (V) conditions do not, however, correspond to the most common experimental conditions and therefore it is often desirable to implement MD simulations in the canonical (NVT) and isothermal-isobaric (NPT) ensembles. An additional reason for preferring the NVT ensemble is that when long run lengths are required, as in the case of studies of slow dynamics in liquids or glasses, there may be significant energy drift in the NVE ensemble.

Two types of approaches have been developed to adapt MD simulations to the canonical ensemble: (i) extended Lagrangian methods, such as Nose-Hoover thermostats and (ii) resampling or rescaling of velocities, as in the case of the Andersen and Berendsen thermostats. The extended Lagrangian methods will generate the true canonical distribution of velocities. The rescaling approaches will only ensure that the average kinetic energy of the system corresponds to the expected value at the desired temperature but have the advantage that they can be combined very simply with the Verlet algorithm. In both approaches, the degree of perturbation of the real time evolution of the system can be adjusted by manipulating various thermostat parameters.

The Berendsen thermostat represents a proportional scaling of the velocities per time step in the algorithm with the scaling factor being given

by

$$\lambda = 1 + \frac{\Delta t}{\tau_B}\left(\frac{T_0}{T} - 1\right) \tag{1}$$

where Δt is the time step, τ_B is the time constant of the Berendsen thermostat , T_0 is the desired temperature and T is the instantaneous temperature [3].The velocity rescaling can be incorporated easily into the Verlet leapfrog algorithm. By varying the thermostat time constant, τ_B, one can, in effect, increase or decrease the degree of coupling to an external bath. The limit, $\tau_B \to \infty$, represents the microcanonical ensemble. The original paper of Berendsen et al applied this thermostatting procedure to simulations of 216 water molecules bound by the rigid SPC potential. Static structural averages were shown to be unaffected for values of τ_B as small as 0.01 ps. Fluctutations in global properties were strongly affected when τ_B was less than 0.1ps implying that analysis of fluctuations cannot be used to determine observable properties. Single-particle properties, including dynamical quantities such as the diffusivity and orientational correlation times, were found to agree, within the limits of statistical error, with the results derived from the microcanonical ensemble for $\tau_B > 0.1$ ps. While the Berendsen thermostat is widely used, we have come across only a limited set of subsequent studies in the literature which inspect in detail the nature of the associated trajectories [4, 5, 6].

In this note, we perform some detailed tests of the effect of the Berendsen thermostat on the dynamical properties of water. The motivation for these tests comes from prior work on molecular dynamics simulations of bulk water where power spectra associated with a number of dynamical quantitites were

shown to possess a $1/f^{\alpha}$ frequency regime, indicative of multiple time scale behaviour due to hydrogen bond network re-organisations [7, 8, 9, 10, 11]. The power spectrum is defined as

$$S(f) = \left| \int_{t_{min}}^{t_{max}} (A(t) - \langle A \rangle) e^{2\pi i f t} dt \right|^2 . \tag{2}$$

where $A(t)$ is any time-dependent mechanical quantity and $\langle A \rangle$ is the corresponding average over the system trajectory. Most recently we have examined power spectra generated from fluctuations in tagged particle quantities sensitive to the local molecular environment, such as the tagged particle potential and kinetic energies, over a wide temperature range [11]. Fluctuations in the tagged particle potential energies, but not in the kinetic energies, were shown to give rise to $1/f^{\alpha}$ noise, indicative of a structural origin for the multiple time-scale behaviour; moreover, the exponents and frequency range of $1/f^{\alpha}$ behaviour were shown to be temperature-dependent. This suggests that the $1/f^{\alpha}$ behaviour of power spectra may provide a simple and convenient way of monitoring changes in the hydrogen bond network dynamics with temperature or density. Since many of the anomalous features of water, originating from its unusual network structure, are more marked in the supercooled regime, it is of interest to study the $1/f^{\alpha}$ behaviour at low temperatures. Molecular dynamics simulations of supercooled water typically require long run lengths of the order of 2ns or more if reliable estimates of dynamical quantities, such as the diffusivity, are to be obtained. The Berendsen thermostat is frequently used to generate the trajectory for such long runs to avoid the energy drift associated with microcanonical runs and facilitate comparison with experimental data [12, 13, 14, 15, 16]. To check

the effect of the Berendsen thermostat on temporal correlations associated with fluctuations in tagged particle quantities, we have carried out a set of tests on a range of state points for SPC/E water.

The potential energy surface of water was represented by the rigid, non-polarizable, three-site SPC/E model [17]. The molecular dynamics (MD) simulations were performed using the DL_POLY software package [2, 18, 19]. A cubic simulation cell containing 256 SPC/E water molecules was used. Electrostatic interactions were evaluated using the Ewald sum approach. The MD trajectory was propagated in the microcanonical (NVE) ensemble using the Verlet leapfrog algorithm in conjunction with the SHAKE algorithm to implement bond constraints [1]. MD trajectories were also generated in the NVT ensemble using the Berendsen thermostat with a range of time constants. In keeping with earlier work, a time step of 1 fs was used for all the simulations and production run lengths were kept at 2ns. The coupling constant for the Berendsen thermostat was assigned values of 1, 10, 25, 50 and 200ps. Table 1 summarises our results from from the NVT and NVE simulations at the following temperatures along the 1 g cm^{-3} isochore: 229K, 260K and 295K. The melting point of SPC/E water at 1 atm pressure is known to be below 260 K [20]. The pressure, P, and the configurational energy, U, correspond to simple thermodynamic averages and the associated errors were estimated by block averaging [21]. The large error bars on the pressure are typical of systems with electrostatic interactions; within statistical error, our results agree well with those in the literature.

We now consider the power spectra generated from fluctuations in the tagged particle potential energies at the different state points (see Figure

1). The tagged particle potential energy, $u(t)$, is defined as the interaction energy of an individual molecule with all the other molecules in the system and the corresponding power spectrum is denoted by $S_u(f)$. Since the potential energy surface is assumed to be pair-additive, the total potential energy, $U(t) = 0.5 \sum_i u_i(t)$ where the sum extends over all molecules. Tagged particle potential energies of 32 molecules in each simulation were sampled at intervals of 10fs and Fourier transformed to generate the power spectra using standard FFT routines [22]. When generating power spectra, a square time window of 328 ps width and a sampling interval of 10 fs was used. This choice of sampling interval corresponds to a Nyquist frequency of 1666 cm^{-1} and sets an upper bound on the frequency range over which we can obtain power spectra. The values of τ_B provide the lower limit on the frequency range over which we can obtain reliable power spectra; thus, τ_B = 1ps corresponds to a lower frequency limit of 33 cm^{-1}. The normalisation convention was chosen such that the integrated area under the $S(f)$ curve equalled the mean square amplitude of the time signal. Statistical noise in the power spectra was reduced by averaging over overlapping time signal windows as well as over individual tagged particle spectra; typically 11 windows were used to cover the 2ns run length. In a given frequency interval showing $1/f^{\alpha}$ behaviour, linear least squares fitting of $\ln S(f)$ was done to obtain the α values with an estimated standard error of less than 3%. Additional computational details regarding calculation of power spectra are given in ref.[11].

Figure 1(a) shows the $S_u(f)$ spectra at 230K obtained from the NVE run as well as from NVT runs with different values of τ_B are shown. At this

temperature, the $S_u(f)$ curve shows three distinct features: (i) a broad peak, originating from librational modes, centred at approximately 600 cm^{-1}; (ii) a $1/f^{\alpha}$ regime between 60 and 298 cm^{-1} and (iii) a second, low-frequency $1/f^{\alpha'}$ region between 1 and 40 cm^{-1} such that $\alpha \neq \alpha'$. On a logarithmic scale, the power spectra obtained from the different simulations are indistinguishable. Careful inspection of the $S_u(f)$ curves, however, shows that the noise in the results obtained with $\tau_B = 25$ps is somewhat larger than in all the other cases. To quantify the effect on the $S_u(f)$ curves, we have tabulated the α and α' values in Table I. The low frequency exponent α' from all the runs agrees to within 3% except at $\tau_B = 25$ps. The spread in the values of the high-frequency exponent α is somewhat larger with again a maximum deviation at $\tau_B = 25$ps. While the deviation at $\tau_B = 25$ps is not large, it is interesting that it should be greater than the deviation seen for the smallest τ_B value of 1ps. The results for 260K, shown in Figure 1(b) and Table I, are very similar in that variations with τ_B values are very small and within the estimated statistical error. The α and α' values are, however, very similar, indicating that it may be better to characterise the region from 1 to 300 cm^{-1} as a single $1/f^{\alpha}$ region. The $S_u(f)$ curve at 295K clearly shows only one $1/f^{\alpha}$ region which merges into the librational band with a crossover to white noise behaviour below 2 cm^{-1}.

In addition to the results shown for the tagged particle potential energy, we have checked the convergence, with respect to τ_B, of power spectra associated with a number of other tagged particle quantities, such as the local kinetic energies and order parameters, and found similar trends to those discussed above. From our results, it is evident that the Berendsen

thermostat preserves the temporal correlations in tagged particle quantities remarkably well over a wide frequency range, even for Berendsen thermostat coupling constants as small as 1 ps but the small discrepancy seen at 230K for $\tau_B = 25$ps does remain. Figure 2 shows the mean square displacement as a function of time at this state point, as an additional check, from the different simulations. On a logarithmic scale, the curves are indistinguishable but it can be seen that the diffusivity estimates obtained at $\tau_B = 25$ps would be slightly different than for all the other cases.

To understand the discrepancy seen for $\tau_B = 25$ps at 230K, we have performed simulations for three additional values of τ_B at 230K and 1 g cm^{-3}; all the tagged particle power spectra are shown in Figure 3. It can be seen that the τ_B values of 25ps and 20ps result in significantly greater noise and change in shape of the $S_u(f)$ curves in the 100 to 400 cm^{-1} regime. These values of τ_B must therefore correspond to some physically significant dynamical time scales of bulk water. The frequencies of the O-O stretching and O-O-O bending modes are at 200 cm^{-1} (0.165 ps) and 50 cm^{-1} (0.66ps) respectively [23]. Clearly all the τ_B values chosen by us lie above the time scales associated with these intermolecular vibrations. In reviewing the literature on the dynamics of supercooled SPC/E water, we found, however, that the time at which the non-Gaussianity parameter is a maximum is 20.6 ps at 224K and 15.5ps at 238K [24]. The time at which the non-Gaussianity parameter peaks is an indication of the time scale on which dynamical correlations are most pronounced. This suggests that anomalous noise effect seen for τ_B values of 20 and 25ps is due to a coincidence of the time scales for the thermostat and for correlated motion in supercooled

water. At higher temperatures, such long-lived correlations are much less pronounced and therefore variations in the power spectra with τ_B are not as noticeable.

Figure 4 shows the power spectra obtained from fluctuations in the total potential energy of the system from NVE and NVT simulations. As expected, these power spectra are much more noisy than those obtained from tagged particle potential energies. Despite the fact that fluctuations in global quantities are expected to be much more subject to distortion on thermostatting than single-particle quantities, the power spectra obtained from the NVT ensemble simulations with $\tau_B = 200$ps agree well with the NVE results for a frequency range of 0.2 to 1000 cm^{-1}. The results for $\tau_B = 1$ps, do, however, show large deviations in the low frequency regime below 10 cm^{-1}.

This study indicates that NVT ensemble simulations using the Berendsen thermostat are successfully able to reproduce the temporal correlations in tagged particle quantities over a very wide frequency range provided sufficiently large values of the Berendsen time constant are used. Even the power spectra associated with global quantities, such as the total potential energy, are well reproduced for frequencies greater than $1/\tau_B$. It is, however, worthwhile to check the dynamical behaviour for a range of thermostat time constants since some values may show slightly larger deviations from microcanonical behaviour than others. This effect is more pronounced on supercooling and is noticeable for values of the Berendsen thermostat time constant which are similar to the time at which the non-Gaussianity parameter is maximum, suggesting that the anomalous values of τ_B fall in the

range of time scales associated with slow structural relaxations. Though the Berendsen thermostat is widely used, we are not aware of any previous study which has demonstrated this effect. We expect that analogous deviations from microcanonical behaviour will be seen with other thermostats when slow relaxation processes are present.

Acknowledgements Financial support for this work has been provided by the Department of Science and Technology (SP/S1/H-16/2000). AM would like to thank the Council for Scientific and Industrial Research, New Delhi for the award of a Junior Research Fellowship.

References

[1] Allen, M. P., and Tildesley, D. J., 1986, Computer Simulation of Liquids (Oxford: Clarendon Press).

[2] Frenkel, D., and Smit, B., 2002, Understanding Molecular Simulation: From Algorithms to Applications (San Diego and London: Academic Press).

[3] Berendsen, H. J. C., Postma, J. P. M., van Gunsteren, W. F., DiNola, A., and Haak, J. R., 1984, J. Chem. Phys. 81, 3684-3690.

[4] Morishita, T., 2000, J. Chem. Phys. 113, 2976-2982..

[5] D'Alessandro, M., Tenenbaum, A., and Amadei, A., 2002, J. Phys. Chem. B 106, 5050-5057.

[6] Lemak, A. S.,and Balabaev, N. K., 1994, Mol. Sim. 13, 177-187.

[7] Nayak, S. K., Ramaswamy, R., and Chakravarty, C., 1995, Phys. Rev. Lett. 74, 4181-4184.

[8] Sasai, M., Ohmine, I., and Ramaswamy, R., 1992, J. Chem. Phys. 96, 3045-3053.

[9] Ohmine, I., 1995, J. Phys. Chem 99, 6767-6776.

[10] Shiratani, E., and Sasai, M., 1996, J. Chem. Phys. 104, 7671-7680.

[11] Mudi, A., Ramaswamy, R., and Chakravarty, C. 2003, Chem. Phys. Lett. 376, 683-689.

[12] Starr, F. W., Sciortino, F., and Stanley, H. E., 1999, Phys. Rev. E. 60, 6757-6768.

[13] Harrington, S., Poole, P. H., Sciortino, F., and Stanley, H. E., 1997, J. Chem. Phys. 107, 7443-7450.

[14] Netz, P. A., Starr, F. W., Stanley, H. E., and Barbosa, M. C., 2001, J. Chem. Phys. 115, 344-348.

[15] Netz, P. A., Starr, F. W., Barbosa, M. C., and Stanley, H. E., 2002, Physica A 315, 470-476.

[16] Scala, A., Starr, F. W., La Nave, E., Sciortino, F., and Stanley, H. E., 2000, Nature 406, 166-169.

[17] Berendsen, H. J. C., Grigera, J. R., and Straatsma, T. P., 1987, J. Phys. Chem 91, 6269-6271.

[18] Smith, W., Yong, C. W., and Rodger, P. M. DL_POLY: Application to molecular simulation. 2002, Mol. Sim. 28, 385-471.

[19] The DL_POLY website is http://www.dl.ac.uk/TCS/Software/DL_POLY/.

[20] Gay, S. C., Smith, E. J., and Haymet, A. D. J., 2002, J. Chem. Phys. 116, 8876-8880.

[21] Flyvberg, H., and Petersen, H. G., 1989, J. Chem. Phys. 91, 461-466.

[22] Press, W. H., Flannery, B. P., Teukolsky, S. A., and Vetterling, W. T., 1990, Numerical Recipes in Fortran (Cambridge: Cambridge University Press).

[23] Parker, M. E., and Heyes, D. M., 1998, J. Chem. Phys. 108, 9039-9049.

[24] Sciortino, F., Gallo, P., Tartaglia, P., and Chen, S.-H., 1996, Phys. Rev. E. 54, 6331-6343.

Figure Captions

1. Comparison of power spectra of the tagged particle potential energy fluctuations from the NVE ensemble and from NVT runs using different values of the Berendsen coupling constant along the 1 g cm^{-3} isochore at (a) 230K, (b) 260K and (c) 295K. Insets show comparison over a relatively small frequency range between the NVE results and the results for a single value of τ_B. The figure key is the same in all cases.

2. Mean square displacement (MSD), in units of $A^{\circ 2}$, as a function of time (in ps) for different values of the Berendsen coupling constant at 230K and 1 g cm^{-3}. Inset shows the data using the logarithmic scale.

3. Comparison of power spectra of the tagged particle potential energy fluctuations from the NVE ensemble and from NVT runs using different values of the Berendsen coupling constant at 1 g cm^{-3} and 230K. The power spectra for different values of τ_B are multiplied by different factors to facilitate comparison of the overall shapes of the curves.

4. Comparison of the power spectra of the total potential energy fluctuations at 295K and 1 g/cm^3 for different values of the Berendsen coupling constant.

Table 1: Summary of simulation results from microcanonical(NVE) and canonical(NVT) ensemble simulations of SPC/E water at state points along the 1 g cm^{-3} isochore. Each run is 2ns long. The error bars on the temperature (T) apply in the case of the microcanonical (NVE) ensemble run. The exponent α is obtained by fitting $S_u(f)$ to a $1/f^{\alpha}$ form over the frequency ranges 60-298 cm^{-1} (230K), 60-298 cm^{-1} (260K) and 4-200 (295K). The exponent α' is obtained by fitting to a $1/f^{\alpha}$ form in the frequency range 1-40cm^{-1} at 230K and 260K.

T (K)	τ_B (ps)	P (MPa)	U (kJ/mol)	α	α'
229.5±0.7	∞	-22±4	-51.3±0.2	1.37	1.18
	200	-17±5*	-51.3±0.2*	1.39	1.16
	50	-15±4*	-51.3±0.4*	1.31	1.16
	25	-23±4	-51.2±0.4*	1.22	1.22
	10	-17±4*	-51.3±0.4*	1.30	1.18
	1	-23±4	-51.3±0.4*	1.36	1.18
260.3±0.6	∞	-24±3	-49.1±0.2	1.30	1.35
	200	-26±3	-49.1±0.2	1.28	1.36
	50	-24±3	-49.1±0.2	1.33	1.35
	25	-24±3*	-49.1±0.3*	1.29	1.35
	10	-26±3	-49.1±0.2*	1.31	1.35
	1	-23±3	-49.1±0.2*	1.34	1.34
295.3±0.4	∞	3±1	-46.9±0.1	1.47	
	200	2±1	-46.9±0.2	1.46	
	50	2±1	-46.9±0.2	1.46	
	25	2±1	-46.9±0.1	1.47	
	10	-1±1	-46.9±0.1	1.46	
	1	1±1	-46.9±0.1	1.46	

Fig 1a

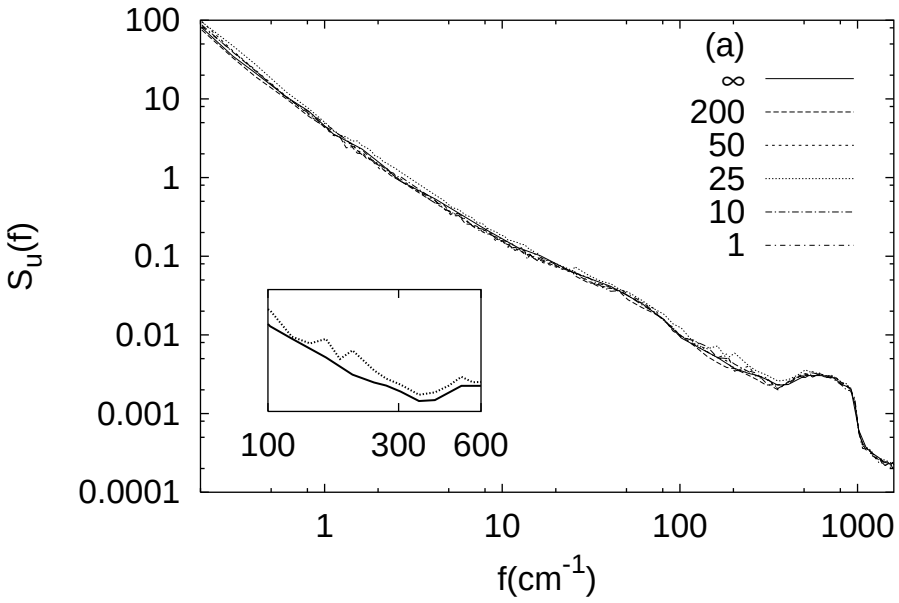
100
10
1
0.1
0.01
0.001
0.0001
$S_u(f)$
1
10
100
1000
f(cm^{-1})
(a)
∞
200
50
25
10
1
100
300
600

Fig 1b

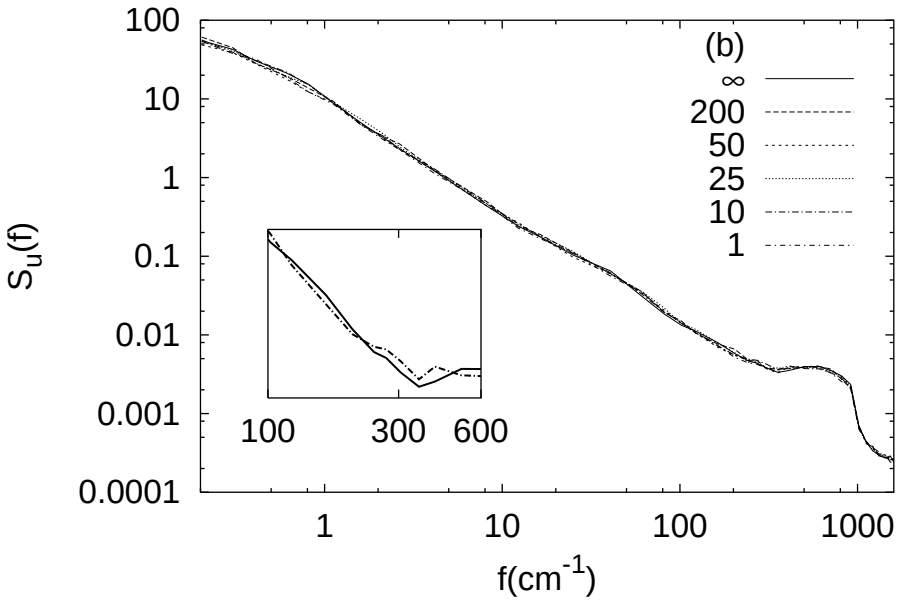
100
10
1
0.1
0.01
0.001
0.0001
$S_u(f)$
1
10
100
1000
f(cm^{-1})
(b)
∞
200
50
25
10
1
100
300
600

Fig 1c

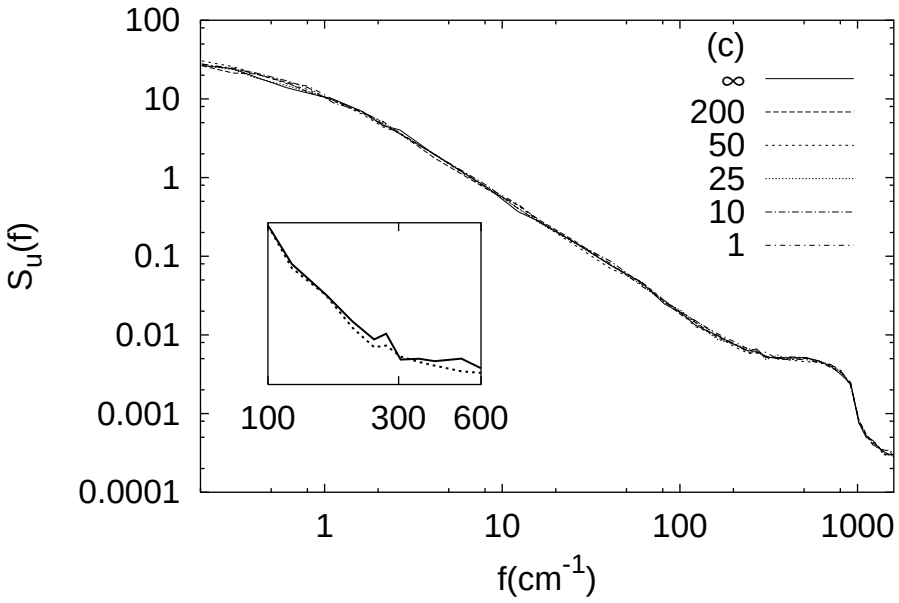
100
10
1
0.1
0.01
0.001
0.0001
$S_u(f)$
1
10
100
1000
f(cm^{-1})
(c)
∞
200
50
25
10
1
100
300
600

Fig 2

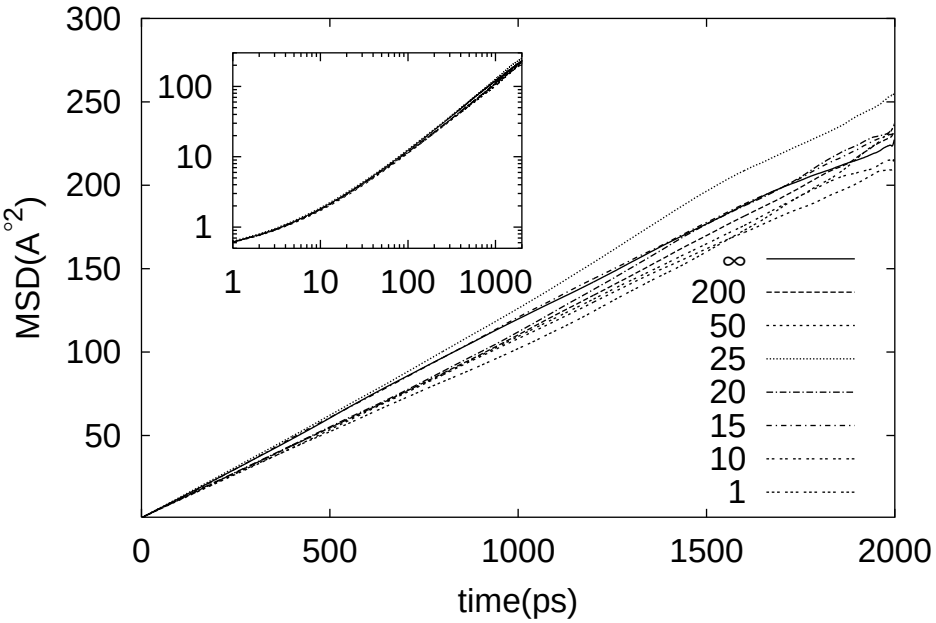
MSD(A°2)
time(ps)
300
250
200
150
100
50
0
500
1000
1500
2000
100
10
1
1
10
100
1000
∞
200
50
25
20
15
10
1

Fig 3

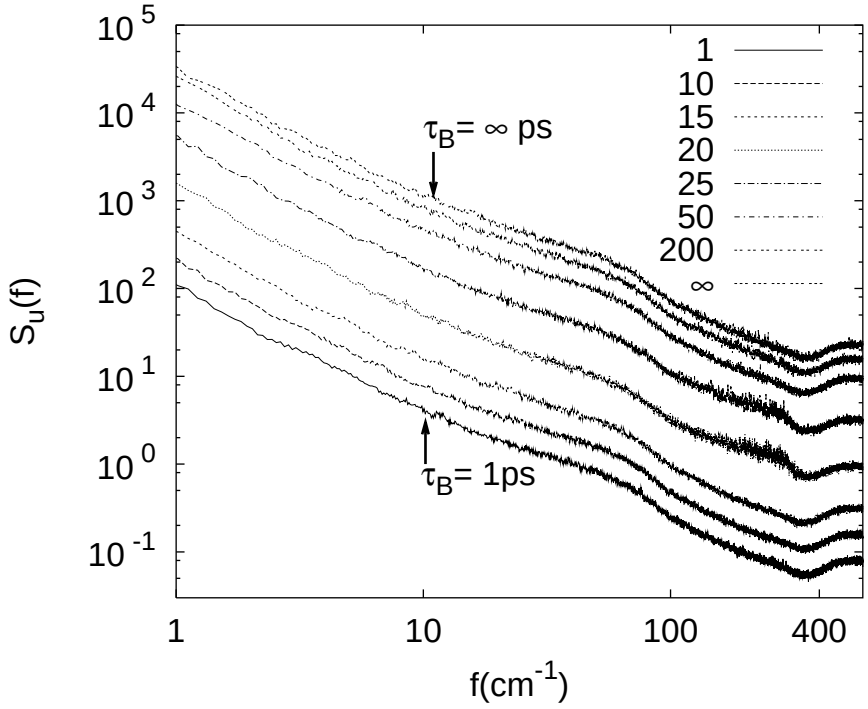
10^5
10^4
10^3
10^2
10^1
10^0
10^{-1}
$S_u(f)$
1
10
100
400
f(cm^{-1})
τ_B= ∞ ps
τ_B= 1ps
1
10
15
20
25
50
200
∞

Fig 4